doi:10.1016/j.jmb.2009.04.062 J. Mol. Biol. (2009) 391, 26–41

JMB

Available online at www.sciencedirect.com

ScienceDirect

ELSEVIER

Structural and Functional Analysis of the Globular Head Domain of p115 Provides Insight into Membrane Tethering

Yu An[1,2], Christine Y. Chen[1], Bryan Moyer[1], Piotr Rotkiewicz[4], Marc-André Elsliger[2], Adam Godzik[4], Ian A. Wilson[2,5]* and William E. Balch[1,2,3,5,6]*

[1]*Department of Cell Biology, The Scripps Research Institute, 10550 North Torrey Pines Road, La Jolla CA 92037, USA*

[2]*Department of Molecular Biology, The Scripps Research Institute, 10550 North Torrey Pines Road, La Jolla CA 92037, USA*

[3]*Department of Chemical Physiology, The Scripps Research Institute, 10550 North Torrey Pines Road, La Jolla CA 92037, USA*

[4]*Program in Bioinformatics and Systems Biology, Burnham Institute for Medical Research, 10901 N. Torrey Pines Road, La Jolla, CA 92037, USA*

[5]*Skaggs Institute for Chemical Biology The Scripps Research Institute, 10550 North Torrey Pines Road, La Jolla CA 92037, USA*

[6]*The Institute for Childhood and Neglected Disease, The Scripps Research Institute, 10550 North Torrey Pines Road, La Jolla CA 92037, USA*

Molecular tethers have a central role in the organization of the complex membrane architecture of eukaryotic cells. p115 is a ubiquitous, essential tether involved in vesicle transport and the structural organization of the exocytic pathway. We describe two crystal structures of the N-terminal domain of p115 at 2.0 Å resolution. The p115 structures show a novel α-solenoid architecture constructed of 12 armadillo-like, tether-repeat, α-helical tripod motifs. We find that the H1 TR binds the Rab1 GTPase involved in endoplasmic reticulum to Golgi transport. Mutation of the H1 motif results in the dominant negative inhibition of endoplasmic reticulum to Golgi trafficking. We propose that the H1 helical tripod contributes to the assembly of Rab-dependent complexes responsible for the tether and SNARE-dependent fusion of membranes.

**Corresponding authors.* E-mail addresses: wilson@scripps.edu; webalch@scripps.edu.

Abbreviations used: ER, endoplasmic reticulum; TRAPP, transport protein particle; COG, conserved oligomeric Golgi; SNARE, soluble *N*-ethylmaleimide-sensitive factor attachment protein receptors; MAD, multiwavelength anomalous diffraction; TR, tether repeat; VSV-G, vesicular stomatitis virus glycoprotein; TC, tethering complex.

Received 13 January 2009;
received in revised form
10 April 2009;
accepted 15 April 2009
Available online
3 May 2009

Edited by R. Huber

Keywords: vesicle transport; membrane trafficking; membrane tethering; p115; membrane fusion

Introduction

The membrane architecture of eukaryotic cells comprising the exocytic (endoplasmic reticulum (ER), Golgi, cell surface) and endocytic (endosomes, lysosomes) pathways is organized by the action of cytosolic and membrane-associated proteins comprising the membrome.[1] Rab GTPase families regulate the dynamic assembly and disassembly of protein complex hubs that integrate membrome component function with vesicle tethering, docking and fusion.[2-4] Tethering is an essential step in membrane trafficking and is now thought to encompass, from a structural point of view, a large group of α-helix-rich, coiled-coiled proteins, the Golgins,[5-14] multi-subunit transport protein particle (TRAPP)[15-20] and conserved oligomeric Golgi (COG) complexes,[21-26] and numerous Rab effectors that contribute to the generation of soluble *N*-ethyl maleimide-sensitive attachment protein receptor (SNARE) fusion complexes.[3,4,22,27-32]

p115 is a tether protein that has been studied extensively.[2,12,33] From rotary shadowing,[34] p115 was suggested to be a myosin-like homodimer with an N-terminal globular head (~70 kDa) and a smaller (~30 kDa) C-terminal, extended coil-coiled domain containing four prototypical, heptads repeats (CC1–CC 4) involved in SNARE assembly[35] terminated by a short acidic domain that auto-regulates Golgi docking events.[36] The yeast homolog of p115, Uso1p, is essential for cell viability, and shows genetic and physical interactions with yeast Rab1 (Ypt1),[34] thereby stressing a key role for p115 in the normal function of the exocytic pathway required for cell proliferation. In mammalian cells, p115 is involved in transport of cargo from the ER to the Golgi, the structural integrity of the Golgi,[33,37-47] and for recovery of the Golgi stack following disassembly during mitosis.[48-50] p115 function is facilitated by interaction with two other Golgin family tethers, GM130 and giantin.[35,39,51-53] Consistent with its cetral role in membrane organization, p115 is a target for apoptotic caspases 3 and 8 that leads to inactivation and fragmentation of the exocytic pathway and amplification of programmed cell death.[54,55] Numerous molecular and biochemical studies suggest that cytosolic p115 is anchored to membranes by the Ras-superfamily GTPase Rab1, and is involved in the assembly of SNARE complexes to promote bilayer fusion.[35,37,43,47,48,56,57] The structural mechanism(s) by which p115 functions to promote tethering and SNARE assembly is unknown. Here, we present the crystal structure of the N-terminal globular domain of the p115 dimer and suggest a role for the N-terminal H1 helical tripod structure in Rab1-mediated ER to Golgi trafficking.

Results

Overall structure

The N-terminal domain of bovine tethering factor p115 ($p115^{Nt}$, residues 1 – 651) was expressed using bacterial systems and purified by Ni-nitrilotriacetic acid (NTA) affinity, ion-exchange, and gel-filtration chromatography (see Materials and Methods). Monomer $p115^{Nt}$ crystallized from a $p115^{Nt}$ monomer pool based on gel-filtration chromatography and diffracted to 2.0 Å. A multiwavelength anomalous diffraction (MAD) data set at 2.7 Å resolution from a selenomethionine derivative was used for the initial phase calculation (Table 1). The $p115^{Nt}$ monomer structure revealed a right-handed, α-solenoid structure composed exclusively of helices and loops (Fig. 1a).[58] The overall shape of the $p115^{Nt}$ monomer corresponds to a bowed cylinder 115 Å long and 55 Å in diameter.

$p115^{Nt}$ crystals were obtained also from a dimer pool of $p115^{Nt}$, based on gel-filtration chromatography, that diffracted to 2.18 Å resolution. The dimer has two molecules in the asymmetric unit, while the monomer structure has one molecule in the asymmetric unit. The dimer assembly is not observed after applying the symmetry operators in the monomer crystals. Superposition of the monomer onto each chain of the dimer did not reveal any major conformational change [root-mean-square difference (rmsds) range from 1.5 Å (main chain) to 1.8 Å (all atoms)]. The $p115^{Nt}$ dimer reveals a Yin and Yang assembly consisting of two single α-solenoids that adopt a left handshake-like structure, with the α-solenoid acting as the palm and an additional helix at the C-terminus, which is disordered in the $p115^{Nt}$ monomer, acting as the thumb in the dimer structure (Fig. 1b and c). The buried surface area of the p115 homodimer interface is 810 $Å^2$ per protomer,[59,60] composed of three distinct sets of residues corresponding to Arg195–Asn243, Glu528–Glu533, and Ser585–Gln595 (Fig. 2). A total of 111 interactions are made in the dimer interface, including 4 salt bridges, 23 hydrogen bonds, and 84 van der Waals contacts (Fig. 2).[61-63] The surface

Table 1. Data collection, phasing and refinement statistics

	Monomer (3grl)	Dimer (3gq2)			
	Native	Se-Met derivative			Native
A. Data collection					
Space group	$C222_1$	$C222_1$			$P2_1$
Unit cell parameters					
a (Å)	155.6	156.4			78.2
b (Å)	174.7	174.6			159.8
c (Å)	87.5	87.4			81.4
β (°)					115.1
Wavelength (Å)		Peak	Inflection	Remote	
	1.000	0.9794	0.9796	0.9537	1.100
Resolution (Å)	50.00 – 2.00 (2.03 – 2.00)	50.00 – 2.70 (2.75 – 2.70)			50.00 – 2.18 (2.25 – 2.18)
Observed reflections	342,057	237,930	238,874	237,523	287,986
Unique reflections	79,589	61,434	61,939	63,557	91,304
Completeness (%)	98.7 (94.6)	99.9 (100.0)	100.0 (100.0)	100.0 (100.0)	96.7 (76.4)
I/σ	34.3 (1.5)	31.6 (5.5)	26.2 (3.9)	18.6 (2.1)	14.3 (1.2)
R_{sym} (%)	4.9 (54.6)	5.2 (24.9)	6.2 (35.0)	9.0 (61.7)	9.1 (59.3)
B. Phasing					
No. sites		12			
FOM after SOLVE		0.53			
FOM after RESOLVE		0.70			
FOM after DM and phase extension		0.60			
C. Refinement					
Resolution (Å)	40.00 – 2.00				20.00 – 2.18
R_{cryst}	17.8				19.9
R_{free}	20.4				25.4
Number of protein atoms	4691				9694
Number of solvent atoms	390				607
Mean *B*-value					
Protein (Å^2)[a]	35.4				31.4
Solvent (Å^2)[a]	41.0				32.3
rmsd from ideal					
Bond lengths (Å)	0.012				0.012
Bond angles (°)	1.25				1.36
Ramachandran plot					
Favored (%)	95.8				93.4
Allowed (%)	3.4				5.1

Values in parentheses are for the highest resolution shell.
$R_{sym} = \Sigma | I_i - \langle I_i \rangle | \ / \ \Sigma | I_i |$ where I_i is the scaled intensity of the ith measurement and $\langle I_i \rangle$ is the mean intensity for that reflection.
$R_{cryst} = \Sigma | \ | F_{obs} | - | F_{calc} | \ | \ / \ \Sigma | F_{obs} |$ where F_{calc} and F_{obs} are the calculated and observed structure factor amplitudes, respectively.
R_{free} = as for R_{cryst}, but for 5.0% of the total reflections chosen at random and omitted from refinement.
[a] These values represent the residual *B* following TLS refinement.

electrostatic potential[64] of the p115 dimer revealed both negatively and positively charged regions (Fig. 1d), potentially reflecting distinct, ligand-binding surfaces. We did not observe density for residues 1–18 for either monomer or dimer crystal structures, suggesting that they may be disordered.

Structurally similar proteins

A search for structurally similar proteins using the Dali server[65] revealed that importin α, a key transport protein in selective nuclear import,[66-68] had the highest similarity to p115 (*Z*-score of 23.0 for subunits of the dimer) (Supplementary Data Table S1). Importin α contains a tandem array of 10 helical, tripod-like, armadillo-consensus sequence repeats, organized in a right-handed α/α/α-solenoid. A high level of similarity was observed for the α-solenoid armadillo repeat of β-catenin,[69] the armadillo-like repeat of the chaperone HspBP1[70] and, more weakly, for importin β, which contains helical-hairpin (α1-loop-α2) HEAT repeats that form an α/α solenoid (Supplementary Data Table S1).[71-73]

Structural organization of p115 repeat motifs

Each subunit of the dimer contains 12 tandem, triple-helical (α1-α2-α3) repeats that forms the right-handed α/α/α-solenoid, referred to herein as the tether-repeat (TR) motif (Fig. 3a, Supplementary Data Table S2). The p115 TR is similar to that of armadillo repeats, despite the fact that each repeat sequence is different, with only the distinct H1 and H2 TR motifs being evolutionarily conserved, suggesting that H1 and H2 TRs have functionally different roles in docking and/or fusion (Supplementary Data Table S2; see below). The first 11 TRs form a continuous right-handed superhelix, and an incomplete C-terminal tether repeat (lacking helix 3) forms

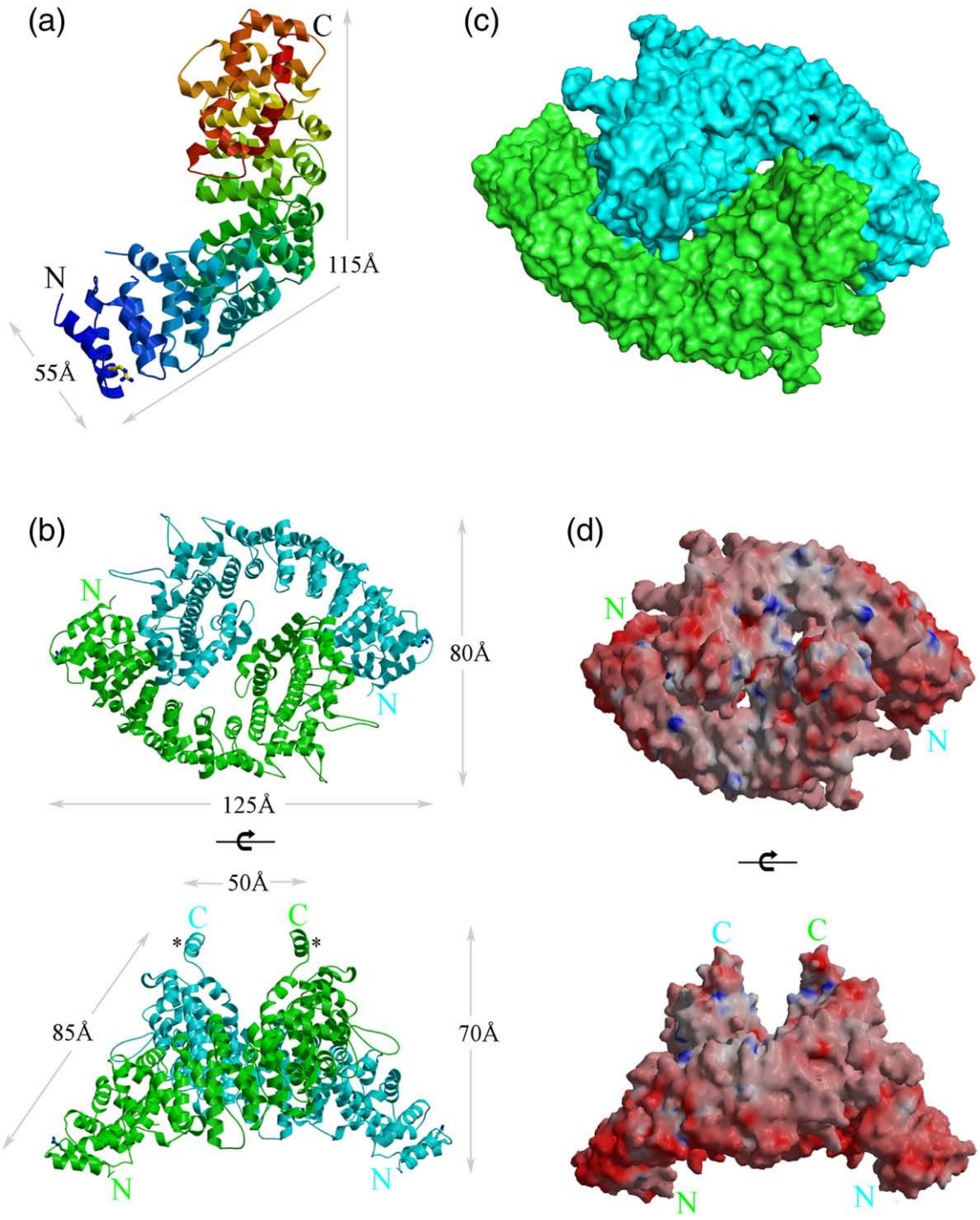

Fig. 1. Structure of $p115^{Nt}$. (a) Overall architecture of the $p115^{Nt}$ monomer in a ribbon representation. The color of ribbon changes from blue to red gradually from the N- to the C- terminus of $p115^{Nt}$. Arg39 involved in stabilization of the N-terminal region is shown in ball-and-stick representation. (b) $p115^{Nt}$ dimer in a ribbon representation. One chain of the dimer is shown in green and the other in cyan. Top view of $p115^{Nt}$ dimer with the C-termini pointing toward the viewer in the upper panel and the side view in the lower panel. The additional C-terminal helix acting as the thumb in the left hand shake-like dimer structure is indicated by the asterisk (∗) in the lower panel. (c) Surface representation of the dimer in the same orientation with the colors as in (b). (d) Electrostatic surface potential of $p115^{Nt}$ dimer. Red surfaces indicate negative potential and blue surfaces indicate positive (±15 kT/e); the top view is in the upper panel, and the side view is in the lower panel. All molecular graphics were prepared with MOLSCRIPT/BOBSCRIPT,[114] Raster3D,[115] or Pymol.[111]

a cap region (Fig. 3a). The $p115^{Nt}$ subunit is composed of TRs that are arranged roughly parallel, with neighboring repeats separated by an average translation of 11 Å. A rotation of approximately 30° (for the first 11 TRs) between adjacent repeats results in a right-handed, superhelical twist along the entire length of the molecule (Fig. 3a). The tight and contiguous packing of the helices leads to an extended

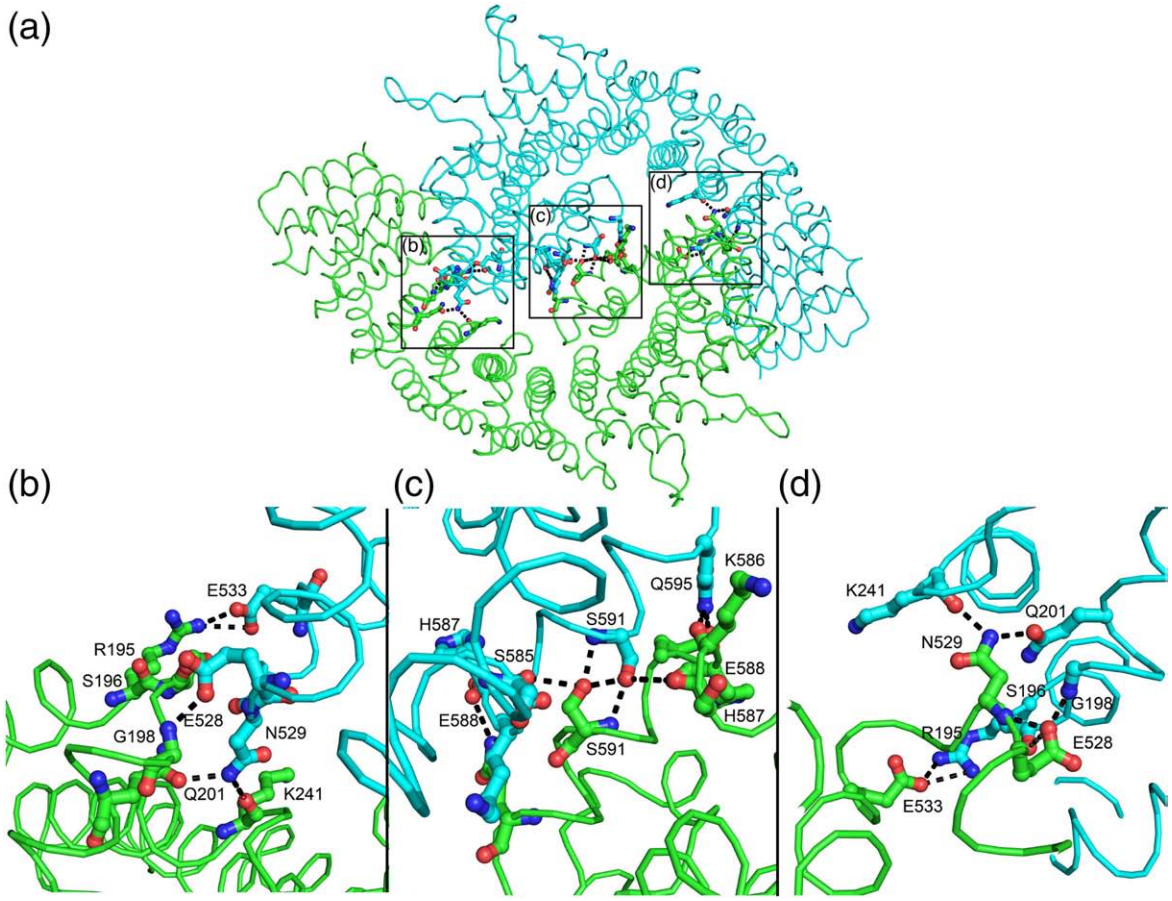

Fig. 2. Salt bridges and hydrogen bond interactions involved in $p115^{Nt}$ dimerization. Hydrogen bonds and salt bridges are shown as broken lines, with interacting residues in ball-and-stick representation.

hydrophobic core along the length of the solenoid. Packing of TRs is further stabilized by hydrogen bonds and salt bridges from hydrophilic residues that are accessible to solvent.

Despite the high degree of variability in the amino acid sequences within each TR, they share very similar overall structures (Fig. 3b). The concave (inner) surface of the p115 N-terminal superhelix is formed from the longest helix (helix 2, yellow) of the 11 TRs. The convex (outer) surface contains more diverse secondary structure elements, including a variety of different length loops and short helices, which are formed primarily from helices 1 (salmon) and 3 (light blue) of the TRs and their connecting regions. The loop insertion between any two adjacent helices varies from 0 to 23 residues, except for the 5th, 8th and 12th TRs, which have additional helical insertions between helices 1 and 2. The rmsds between pairs of TRs range from 1.1 Å to 3.2 Å (main chain). Superimposition of TRs 1–11 (Fig. 3c) reveals a remarkably conserved structural fold comprising a helical tripod (rmsd 1.87 Å, main chain). The incomplete TR found at the C-terminus also follows the right-handed, superhelical twist formed by previous 11 TRs, but with a rotation of approximately 75° instead of 30° for the 11th TR (Fig. 4). This incomplete TR is stabilized through extensive interactions with the concave (inner) surface (helix 2) of tether repeats 8, 9, 10 and 11, which results in this motif acting as a C-terminal cap region of the superhelix formed by the previous 11 TRs, and provides a means to link to the extended coiled coil, the C-terminal region of p115 (residues 652 – 961), likely via a linker region (residues 666–700) that exhibits a low coiled-coiled propensity (PAIRCOIL2).[74,75]

Sequence diversity in the TR structural motif

Each TR consists of 32–44 residues that form three helices; helix 1 consists of 9–14 residues, helix 2 14–21 residues and helix 3 7–15 residues(Supplementary Data Table S2). Variable leucine-rich motifs present in each TR correspond roughly to $x_nLLx_{1-2}LLx_{1-2}LLx_n$ for helices 1 and 2, and x_nLLx_n for helix 3, where x_n can be up to 23 residues for connections between helices, and L represents obligate hydrophobic residues whose side chains point into the solenoid (Fig. 3; Supplementary Data Table S2). These conserved hydrophobic residues can include Leu, Ile, Cys, Ala, Val, Gly, Met, Phe and Pro. The organization for each of the p115 TRs can be identified weakly by using the conserved residues of the armadillo-consensus repeat (Supplementary Data Table S2), but are sufficiently divergent to be defined as armadillo-like TRs that contribute to the

formation of right-handed α/α/α-solenoids. Despite the lack of sequence conservation, the variable, leucine-rich motifs that define the p115 TRs can be detected in a number of tethering protein family members (see Discussion; Supplementary Data Table S2).

The H1 TR motif directs p115–Rab1-GTP complex formation

p115 contains two sequence-conserved regions that, from a structural perspective, can be referred to as the H1-TR (residues 21–54) and the H2-TR (residues 200–252), with yeast Uso1p being the most divergent member (Fig. 5). Glu201 and Lys241 in the H2 region contribute to the stability of the dimer interface (Fig. 2). Previous biochemical studies utilizing monomeric forms of the N-terminal domain of p115 (residues 1–651) did not detect Rab1 binding to the globular head domain.[35,36] In contrast, we found that Rab1-GTP, but not Rab1-GDP, bound strongly to the full-length p115 dimer and to the dimeric form of the $p115^{Nt}$ globular domain, but not to monomeric $p115^{Nt}$, based on gel-filtration chromatography, with the latter result being consistent with previous reports (Fig. 6a).[35,36]

To further assess the potential role of residues in the evolutionarily conserved H1 TR motif involved in Rab1-GTP binding, we mutated selected charged residues in the H1 TR and expressed recombinant $p115^{Nt}$ protein for analysis of binding *in vitro* (Figs. 3 and 6b). Mutation of Arg39 in helix 2 to Glu (R39E) completely disrupted Rab1-GTP binding *in vitro* to full-length p115, a result consistent with its orientation and key role in structural stabilization of the H1 helical tripod (Fig. 6b). Interaction with Rab1-GTP was partially disrupted by mutation of Arg29 to Glu (R29E) in helix 1 facing the solvent on the face opposite the interface between helix1 and helix2 (Fig. 6b). Thus, the N-terminal H1-TR can confer Rab1 interaction *in vitro*. Interestingly, mutation of Glu21 to lysine, which was recently shown to disrupt the interaction between p115 and the COPI β-subunit of the COPI coat complex, [76] had no effect on Rab1 interaction *in vitro*, suggesting that H1 has an additional binding site for other proteins, or that COPI β has a sequence or structural motif similar to Rab1 (Fig. 6b).

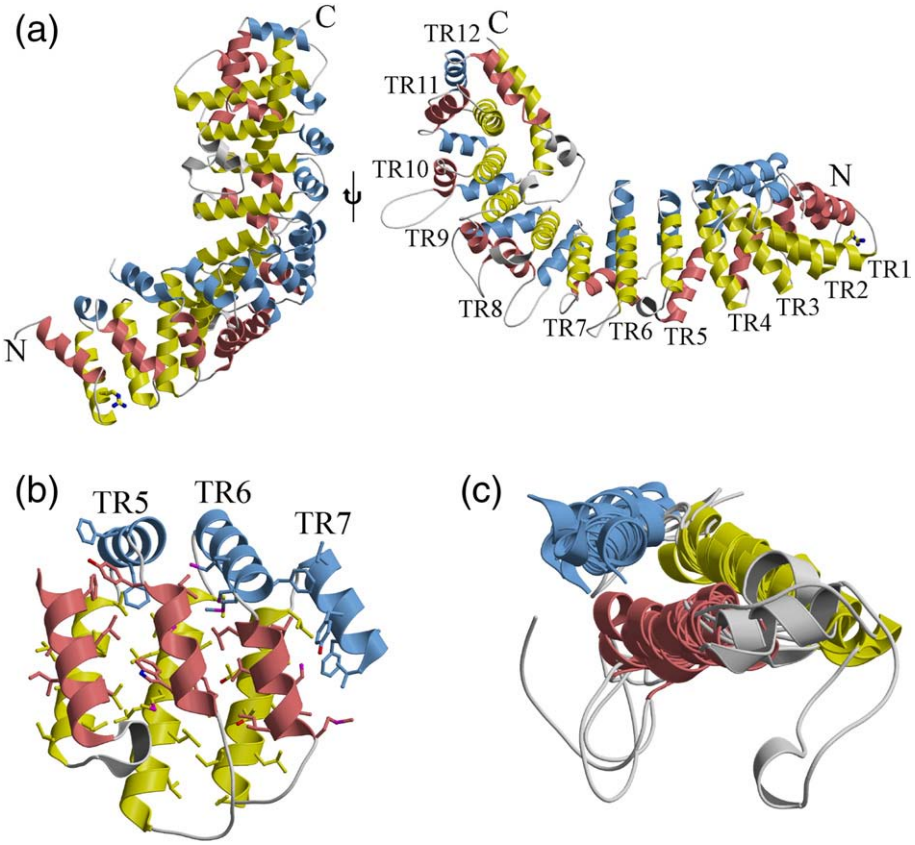

Fig. 3. Tether repeat (TR) motif. (a) Structural features of the 12 TRs in the $p115^{Nt}$ monomer. Except for the C-terminal TR, each TR includes three α-helices, which are shown in salmon, yellow and light blue, respectively. The insertions between any adjacent helices are colored gray. Arg39 is shown in ball-and-stick representation; the side view is in the left-hand panel, and the top view is in the right-hand panel. (b) The conformation of three adjacent tether repeats (TR5, TR6, and TR7) highlights the tight packing of the conserved hydrophobic core throughout the solenoid, where the hydrophobic residues involved in stabilizing the solenoid are shown in ball-and-stick representation. (c) Superimposition of the three 12 TR motifs from the dimer and monomer $p115^{Nt}$ structures show the structural conservation.

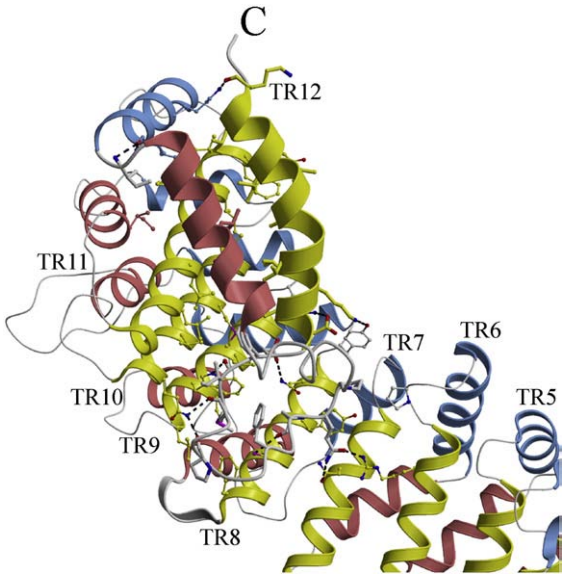

Fig. 4. Conformation of the incomplete tether motif at the C-terminus of $p115^{Nt}$. The 12th TR motif is shown in thicker ribbon representation than other tether repeats where it functions as a C-terminal cap for the α-solenoid. Residues involved in stabilization of the helical domains and the connecting loops of TR12 are represented by ball-and-stick figures. Hydrogen bonds are indicated by broken lines.

The H1 TR is required for ER to Golgi traffic

To test whether the H1 TR is involved in Rab1-dependent trafficking of cargo between the ER and the Golgi, we examined whether p115 H1 TR mutants, which would likely function as dimers, given the extensive C-terminal interactions, could function as dominant negative inhibitors of trafficking. For this purpose, mutants were over-expressed in cells expressing vesicular stomatitis virus glycoprotein (VSV-G), a type 1 transmembrane protein that is efficiently transported between the ER and the Golgi in a p115-dependent fashion. [36,37,39,46,56,77] Overexpression (~10-fold), using a vaccinia transient expression system in the presence of the Sar1-H79G dominant negative mutant that inhibits COPII vesicle formation,[78,79] prevents the export of VSV-G from the ER and acquisition of endoglycosidase H (endo H) resistance, a hallmark of processing by *cis* Golgi α-mannosidases and glycosidases (Fig. 6c).[80-82] Over-expression of the N-terminal (1–650) or C-terminal p115 domains (651 – 960) (data not shown) or full-length p115 protein (Fig. 6c) had little effect on VSV-G trafficking from the ER to the Golgi, as indicated by acquisition of endo H resistance, suggesting that the intact protein is required for function and that excess p115 does not inhibit the activity of interacting components likely functional at the bilayer. Moreover, neither over-expression of single mutants that were tested for interaction with Rab1 *in vitro* (Fig. 6b) (and data not shown), nor deletion of the H1 TR motif (residues 20–60) from the full-length protein, generated a dominant negative phenotype (Fig. 6c). The inability of the R39E mutation to bind Rab1 (Fig. 6a) is consistent with the inability of this mutant to function as a dominant negative inhibitor, particularly if recognition of Rab1 through the H1 motif is the first step in p115 recruitment to membranes. These results suggest that a dominant negative interaction cannot arise by complete ablation of the Rab1 binding site. In contrast, mutants that may partially perturb the interaction of the H1 domain with Rab1 without disrupting the structural organization of the H1 domain (see Discussion) may show a dominant negative phenotype. Indeed, mutants harboring the R29V-S33V-D37V-D38V-N41V combination showed a strong dominant negative effect on VSV-G processing to the endo H resistant form (Fig. 6c). Analysis of binding of this mutant to Rab1 *in vitro* (Fig. 6b) was not possible, given its poor expression in *Escherichia coli*. Because mutants expressing the R29V-S33V or D37V-D38V-N41V combinations were not dominant negative *in vivo* (Fig. 6c), we conclude that residues 29 – 41 provide a platform involving both α1 and α2 helical domains for interaction with Rab1 and possibly other factors. The H1 tripod may facilitate the assembly and/or disassembly of tethering-fusion complexes in ER to Golgi trafficking and Golgi integrity.

Discussion

Structural basis for p115 tether function

We have demonstrated that the evolutionarily conserved tether p115 has a N-terminal head domain assembled from α-helical tripod TRs. The p115 TR α-solenoid is structurally related to the well-studied, superhelical α-solenoid importin α, and β-catenin proteins that are constructed of tri-helical armadillo repeats.[69,72,83] Importin α belongs to a large family of related proteins that serve as adaptors for targeting many proteins to the nucleus.[84] Importin α is a monomeric helicoidal protein, and binds protein ligands through conserved basic nuclear localization signals to its highly flexible internal and external α-helical faces.[85,86] Similarly, monomeric β-catenin utilizes its α-helical faces to organize the assembly of complexes involved in cell signaling.[83,87] In contrast, p115 forms a dimeric helicoidal protein where the internal faces are largely restricted to maintaining an energetically stable dimer interface in the cytosol. Thus, p115 has utilized the interaction surface of the helicoidal head domain to largely limit interactions to its external faces, of which only two TRs, H1 and H2, are highly conserved. Intriguingly, the H2-TR has recently been proposed to bind the conserved oligomeric Golgi (COG) complex.[23] COGs are multimeric complexes that are believed to have a critical role in Golgi structure and retrograde trafficking of a number of Golgi glycan processing enzymes.[25] Disruption of COG function leads to a number of inherited glycosylation disorders.[21] While we found

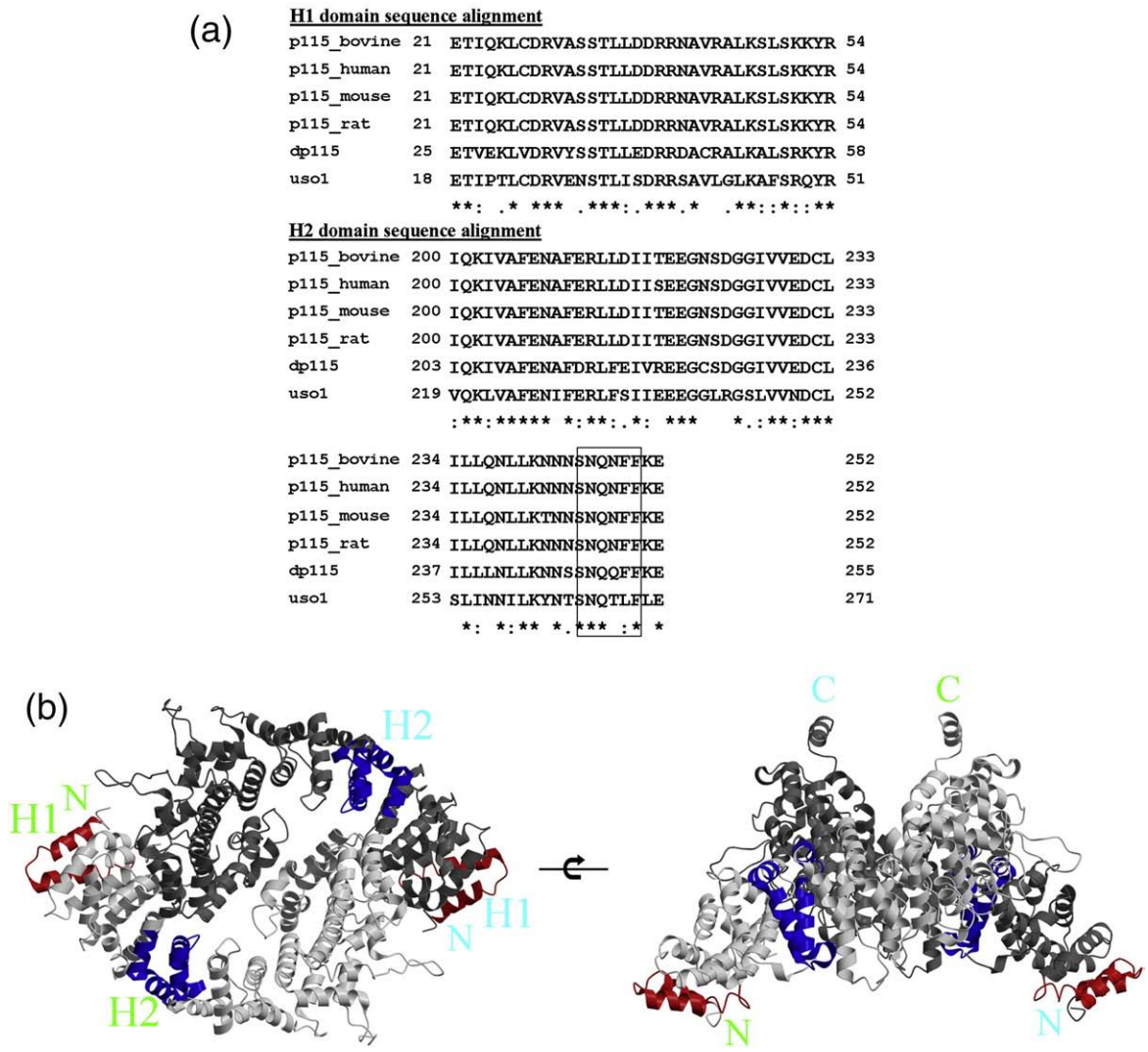

Fig. 5. Sequence alignment and structural orientation of p115 conserved subdomains H1 and H2. (a) Sequence alignment of H1 and H2 regions. While yeast Uso1p (uso1) is more divergent than that observed within higher eukaryotes, its level of conservation suggests significant overlap in functional properties related to the function of domains H1 and H2 in vesicle trafficking. (b) Location of H1 and H2 domains in the p115 dimer structure, with H1 and H2 shown in red and dark blue, respectively; the top view is shown in the left-hand panel, and the side view is shown in the right-hand panel.

that over-expression of a variety of mutants in the H2 domain had no dominant effect on VSV-G transport to the Golgi (data not shown), complete deletion of the H2 domain results in Golgi fragmentation and reduction in ER to Golgi transport,[23] consistent with an important role for both of the conserved H1 (shown herein) and H2[23] domains in p115 function.

While H2 binds COG,[23] we found that the N-terminal H1 TR can bind Rab1. Previous observations demonstrated that Rab1 binds to a coiled-coil region (CC1) (residues 650–961) that lacks predicted TRs and is distal to the N-terminal globular domain reported here.[35] This CC1 domain (residues 650–780) is thought to form a cryptic binding site masked by the acidic tail domain (residues 875–920) that, in the absence of the Golgin tether GM130, displaces the acidic domain and would prevent Rab1 binding.[36,77] Interaction of Rab1 with a coiled-coil domain is not unlike the recent structural complex reported for the yeast Sec4 Rab GTPase bound to a coiled-coil motif in the Sec4 GEF,[88,89] or Rab6 interaction with GCC185.[7] Interestingly, the CC1 region was inactive in Rab1 binding when isolated as a monomeric CC1 fragment.[35] One possibility is that the CC1 region may function only as a dimer, as observed for Rab1 binding to the N-terminal globular domain here. It is possible that both the Rab1 and CC1 interaction domains in the monomeric state are more unfolded and/or flexible in solution when compared to the dimer and, therefore, unable to productively bind Rab1. The identification of the H1 TR domain as a binding partner for Rab1 raises the possibility that two different Rab1 binding regions may have different functions in the sequential events that direct tethering and SNARE assembly, which facilitate vesicle docking and fusion.[35,36,77,90,91] We suggest that the H1 domain may initiate these events, given the complexities associated with GM130 exposing the CC1 motif.[36,77] Although the

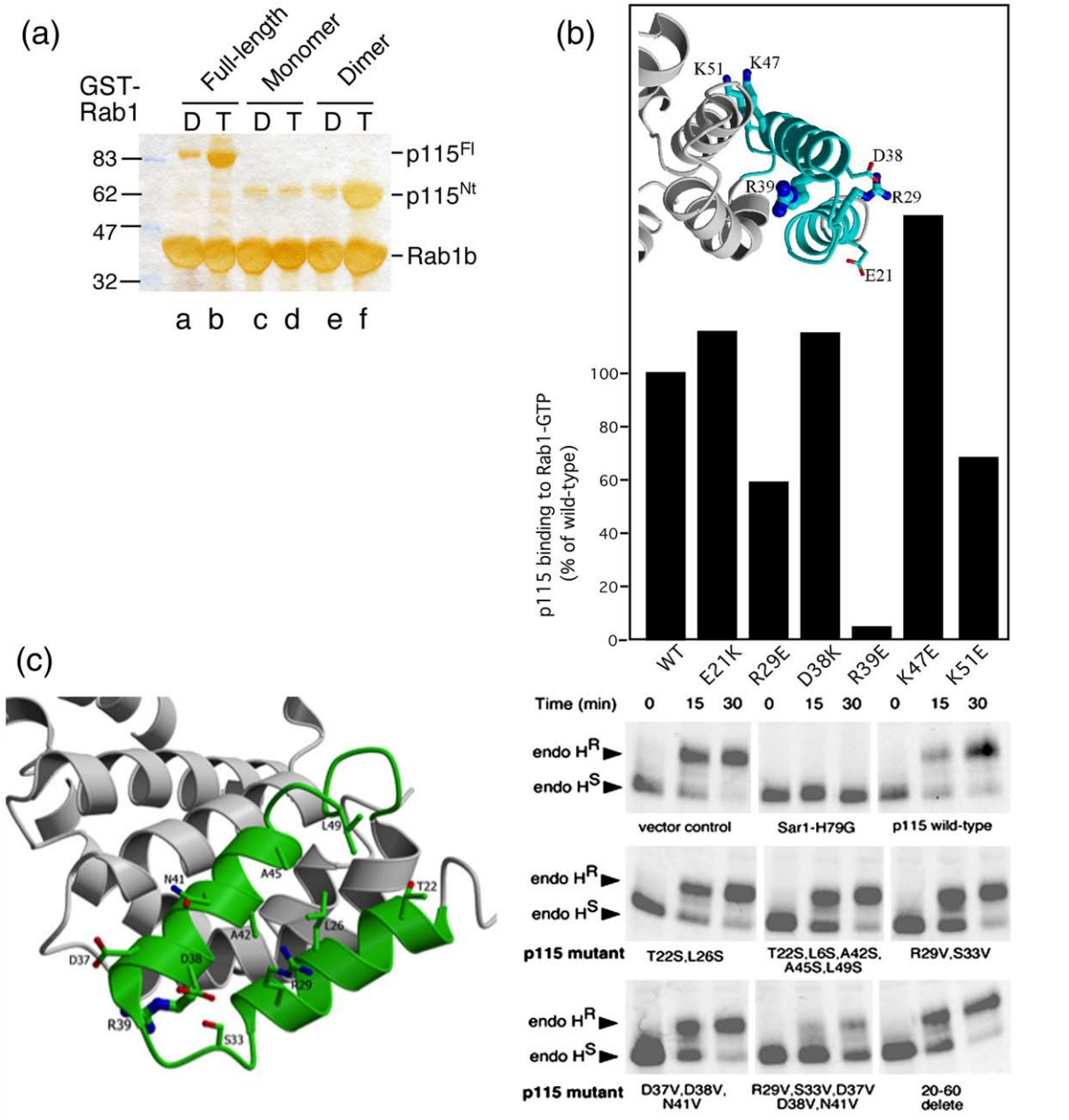

Fig. 6. Role of H1 TR in Rab1 function in ER to Golgi trafficking. (a) Binding of Rab1-GTP, but not GDP, to the full-length p115 dimer and to the dimeric form of the $p115^{Nt}$ globular domain, but not to monomeric $p115^{Nt}$. GST-Rab1-GDP (control; lanes, a, c, and e) and GST-Rab1-GTP bound to GST-beads (lanes b, d, and f) were incubated with recombinant full-length wild type ($p115^{Fl}$; lanes a and b) and mutant monomer (lanes c and d) or dimer (lanes e and f) $p115^{Nt}$ as described in Materials and Methods. A silver-stained gel is shown of Rab1 (lanes a–f), $p115^{Fl}$ (lanes a and b) or $p115^{Nt}$ (lanes c–f) retained on beads. (b) The effect of mutation of H1 residues on Rab1 binding to $p115^{Fl}$. p115 mutants were generated and $p115^{Fl}$ interaction with Rab1 was performed as described in Materials and Methods. p115 binding is reported as a percentage of total wild type $p115^{Fl}$ bound relative to total GST-Rab1 coupled to beads. Inset: Structural orientation of residues mutated for biochemical studies are shown in ball-and-stick representation. (c) Effect of mutations in p115 (left-hand panel) on trafficking of VSV-G (right-hand panel). Transport of VSV-G from the ER to the Golgi was followed by pulse–chase with [^{35}S]Met for the indicated length of time and treatment of cell lysates with endoglycosidase (endo) H followed by SDS-PAGE, as described in Materials and Methods. The reduction of processing to the endo H resistant glycoform reflects decreased delivery to Golgi compartments. Sar1-H79G, or the indicated wild type or mutant full-length p115 construct was over-expressed ~10-fold relative to endogenous p115 using a vaccinia transient expression system, as described in Materials and Methods.

Glu21 residue in the H1 TR has recently been reported to interact with the β-subunit of COPI,[76] we were unable to detect an effect of mutating this residue on the interaction with Rab1. This is consistent with the fact that the Rab1-H1 interacting domain likely involves residues 29–41.

While TRs define the α-solenoid structural organization of the N-terminal globular head domain,

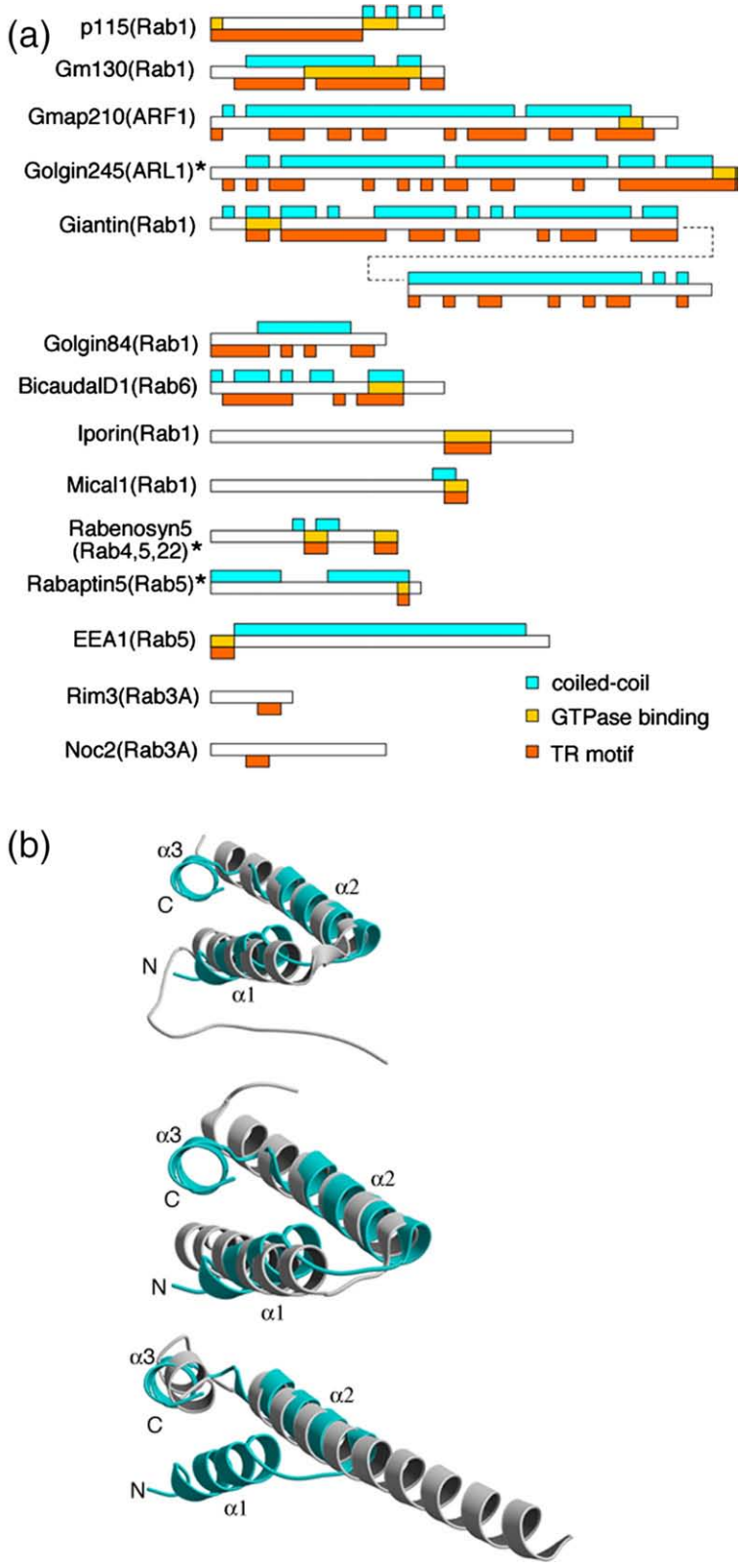

Fig. 7. Conservation of TR structure. (a) Predicted coiled-coil regions are shown in cyan boxes above each protein (with its binding partner); putative TR-containing regions (see Discussion for further details; and see Supplementary Data Table S2) that overlap with predicted coiled-coil regions, are shown in orange boxes below each protein. The region binding ARL1, ARF1 or Rab GTPases is shown by the gold boxes within the protein. An asterisk (∗) indicates TR motifs with known structure. (b) Superimposition of TR motifs of $p115^{Nt}$ and structurally characterized Rab GTPase effector complexes: (upper panel) helices 1 and 2 in the H1 TR of $p115^{Nt}$ (cyan) with Rabenosyn-5 (441-501, PDB 1ZOK) (gray); (middle panel) helices 1 and 2 in the H1 TR of $p115^{Nt}$ (cyan) with Rabenosyn-5 (734-784, PDB-1ZOJ) (gray); and (lower panel) helices 2 and 3 in H1 of $p115^{Nt}$ (cyan) and Rabaptin5 (804-849, PDB-1TU3) (gray).

they lack sequence conservation except for notable leucine-rich motifs that can be best described as armadillo-like features (Supplementary Data Table S2). Although an extensive database analysis using a variety of current alignment algorithms failed to reveal a consensus motif that could be used to define a TR family/superfamily (P.R. & A.G., unpublished results), it is of note that, upon visual inspection, a leucine-rich pattern separated by sequences of variable length, as found for $p115^{Nt}$, can be detected in a broad spectrum of tether proteins that are involved in exocytic and endocytic trafficking pathways (Supplementary Data Table S2). While it is difficult to assign statistical significance to such

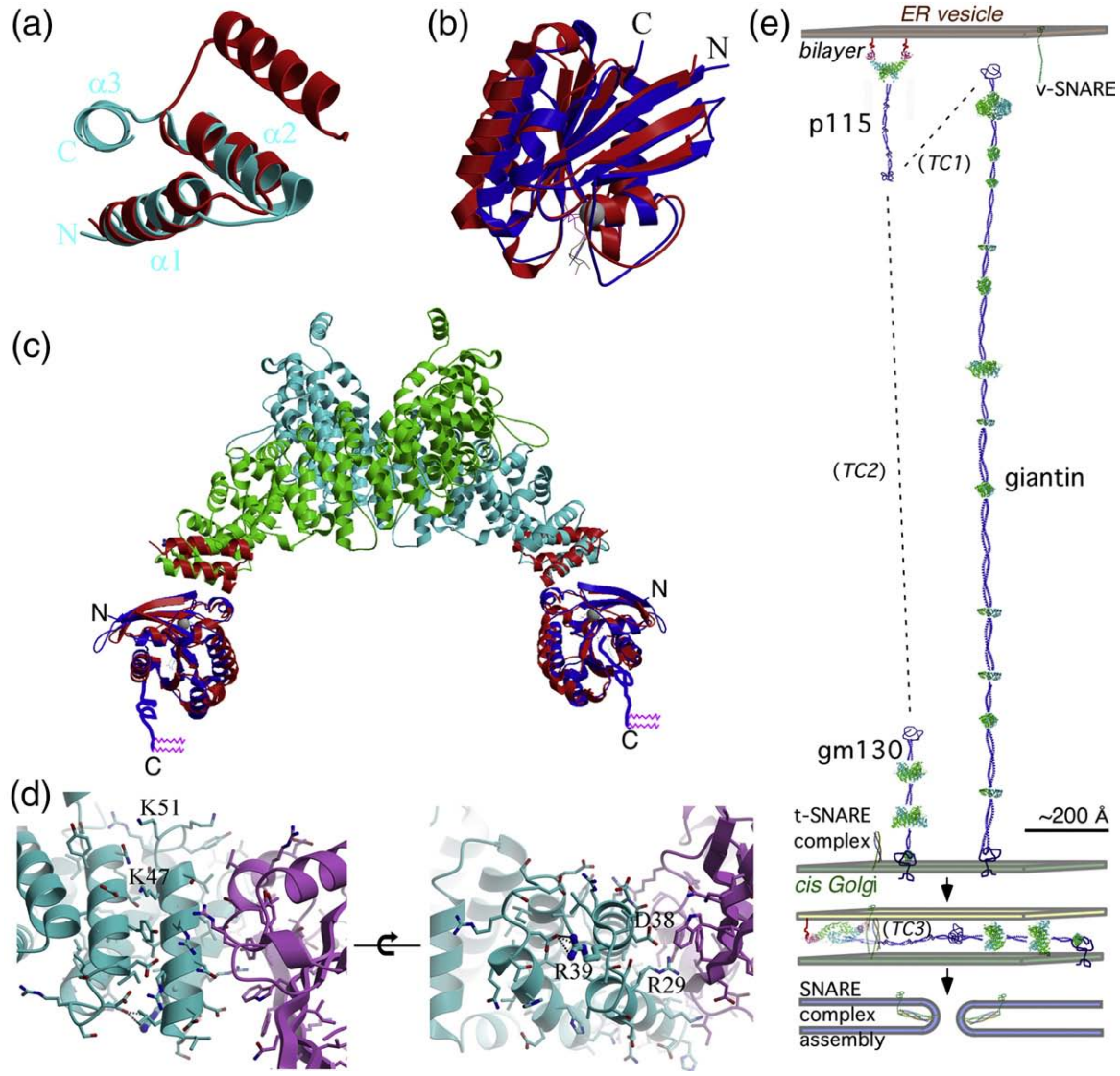

Fig. 8. A model of the Rab1-GTP–p115 complex in membrane tethering. (a) Superimposition of helices 1 and 2 of the TR like-motif in GRIP domain (red) (from the ARL1–GTP–GRIP complex, PDB 1R4A) with H1 of $p115^{Nt}$ (cyan) based on superimposition of consensus hydrophobic residues. (b) Superimposition of ARL1-GTP and Rab5-GTP (PDB 1TU3), with ARL1-GTP (red) and Rab5-GTP (blue). The switch and interswitch regions that interact with the GRIP or H1 TR motifs are facing the viewer. (c) Superimposition of the ARL1(GTP)-GRIP (PDB 1R4A) (red) with the H1 domain of $p115^{Nt}$ and Rab5-GTP (PDB 1TU3) (blue) illustrating a possible molecular model for the Rab1-GTP–p115 complex. The unstructured 23-residue hypervariable domain of Rab1 containing two C-terminal geranylgeranyl prenyl lipids (purple) is indicated with blue lines. (d) Rab1-GTP–p115 complex interface. The Rab1-GTP model (purple) was generated by mutation of corresponding residues of Rab5-GTP (cyan) on the basis of sequence alignment. The indicated residues in p115 were mutated for analysis of their effects on Rab1 binding, as described in the text. Mutation of Asp38 to Lys had no effect on Rab1 binding (Fig. 6b), consistent with its orientation in the homology model. In contrast, while Arg39 does not have direct interactions with Rab1, it is likely required for stabilization of the H1 TR domain and thereby strikingly disrupts interactions with Rab1 when mutated (Fig. 6b). Arg29 likely interacts with the switch regions to alter Rab1 binding (Fig. 6b). Lys47 and Lys51 may affect stabilization of the TR1 domain and have differential effects on Rab1 binding (Fig. 6b). (e) Structural model of p115 ER-Golgi tether-fusion pathway. Binding of p115 by Rab1-GTP[37,45] to the bilayer through the C-terminal prenyl lipids of Rab1 links p115 to ER to Golgi transport vesicles.[37,38] The first step in recognizing the Golgi at a distance is by interaction with the Golgi-associated, extended tether giantin to form tethering complex 1 (TC1) through interaction with the acidic-C-terminal domain of p115.[36,51,99,116] In the subsequent tethering complex (TC2), p115 is bound to the more compact, Golgi-associated GM130 tether, again through the p115 acidic C-terminal domain.[35,39,99] Close juxtaposition of the vesicle bilayer to the Golgi bilayer by TC2 promotes SNARE assembly (TC3) and fusion.[35,37,43,57] The molecular and biochemical events directing transitions between TC1-3 are unknown. p115, giantin and GM130 were structurally modeled on the basis of the distribution of potential TRs (green and cyan icons based on Supplementary Data Table S2) and predicted coiled-coiled motifs. The v-SNARE and t-SNARE partial and complexed structures are illustrated based on the intact SNARE complex (PDB 1N7S). All protein components illustrated are calibrated approximately to their predicted physical dimensions.

manual assignments, it is interesting to note that the leucine-rich pattern separated by sequences of variable length are found nearly exclusively in predicted coiled-coiled regions[74] of Golgins and other Rab effectors where binding to Rab, Arf, and Arl GTPases has been demonstrated.[28] One possibility is that these regions, despite our current inability to recognize them computationally, comprise a broad family of evolutionarily related, α-helix-rich subdomains that adopt structural features to facilitate GTPase-regulated membrane trafficking. The presence of both di-helical and tri-helical interaction domains found in a number of Rab-effector complexes is consistent with this hypothesis (Fig. 7b; Supplementary Data Table S2).[28] Here, two out of the three α-helices appear to be involved in generating a GTPase-binding platform, whereas the third helix contributes to structural orientation of the platform. These differences suggest that GTPase interaction with tethering components can involve a multiplicity of structural motifs, involving α-helical domains, that may have different functional consequences.[92]

Homology model of the Rab1–p115 complex

The structure of the small GTPase ARL1 bound to the C-terminal, α-helix-rich fragment corresponding to the GRIP domain in the tether Golgin 245 has been determined.[93,94] Like Rab1, ARL1 belongs to the Ras superfamily of GTPases that retains a highly conserved core fold that is augmented with unique switch and interswitch regions that direct specific function.[95-97] We performed a structural alignment of the p115 H1 TR with the Golgin 245 GRIP domain bound to ARL1 (PDP codes 1R4D, 1UPT).[93,94] Superimposition of consensus hydrophobic residues of the α1 and α2 helices of the GRIP domain with the α1 and α2 helices of $p115^{Nt}$ H1-TR yielded an rmsd of 0.8 Å (main chain), which indicated similar structural configurations (Fig. 8a). Because ARL1 and Rabs have nearly identical core GTPase folds that bind guanine nucleotide, we were able to align the Rab5 nucleotide binding domain (PBD code 1TU3) with that of ARL1 (PDB code 1R4D) (Fig. 8b). By substitution of the Rab5 switch domain residues to the corresponding Rab1 switch region residues, we could generate a model for the $p115^{Nt}$-Rab1 complex (Fig. 8c) that illustrated the role of R39 in stabilizing the structure of the H1 TR, and R29, and potentially D38, for interaction with Rab1 (Fig. 8d). This alignment yields an orientation consistent with the interpretation that the switch and interswitch regions of Rab1 are involved in binding the H1 TR in p115. The orientation of the truncated C-terminus of Rab1 (Fig. 8c) suggests that binding of either one or two Rab1 molecules to the lipid bilayer can be readily accommodated by insertion of the prenyl lipids covalently attached to conserved cysteine residues at the C-terminus (Fig. 8e).

Our knowledge of the structure of the globular head region, combined with the extensive biochemical analysis of p115 function in trafficking and SNARE assembly,[37-41,43,44] provides an opportunity to model the membrane tethering and docking events in ER to Golgi trafficking that involve p115 (Fig. 8e). p115 is recruited to activated Rab1-GTP on the donor vesicle through the H1 TR domain and likely is retained on the bilayer by the flexible 23 residue, hypervariable, prenylated C-terminus of Rab1.[98] Because p115 interacts with the highly elongated tether giantin that is attached to the acceptor *cis* Golgi compartment,[51,99,100] we raise the possibility that tethering can initially occur at a distance of up to 200 nm from the bilayer. Following this step, p115 may be handed on to the more structurally compact GM130 tether (Fig. 8e).[35,37,39,57] This would serve to physically draw the membrane surfaces together, and, based on current models,[35,77] is expected to accelerate the release of the autoinhibitory acidic domain found at the C-terminus of p115 to allow interaction with Rab1 on the acceptor membrane with the CC1 region of p115, thereby stabilizing association of opposing membranes.[35-38,77] This physical model of tethering explains the observation that, while giantin and GM130 are regulatory, they are not essential for either Golgi assembly or ER to Golgi transport.[42,56,99] Rather, tethering at a distance may improve the overall efficiency of trafficking in higher eukaryotes by reducing a 3D walk in the cytosol to a more restricted 2D walk along the surface of the Golgi.[101] Finally, p115-dependent SNARE assembly at the CC1 region would direct bilayer fusion (Fig. 8e). We conclude that the dimeric solenoid structure of the N-terminal region of p115 described here provides a Rab1-dependent binding platform on the nascent vesicle to initiate a cascade of tethering-fusion events culminating in the transfer of cargo between the ER and the Golgi.

Materials and Methods

Preparation of monomer and dimer p115 N-terminal domains

The N-terminal domain of bovine p115 from residue 1–651 was cloned into the pET-28a vector. The protein was expressed with *E. coli* strain BL21 (DE3) cell and purified using Ni-NTA (Qiagen), ion-exchange (Mono Q, Pharmacia), gel-filtration chromatography (Superdex 200, Pharmacia) and thrombin digestion. The purified protein was concentrated to 10 mg/ml in 50 mM Tris–HCl, pH 8.5. Se-Met protein was expressed with B834 (DE3) cell in Se-Met-containing minimal medium, and purified under reducing conditions, containing 10 mM β-mercaptoethanol. The protein used to prepare the p115 dimer was generated as described for the monomer, with the exception that the protein was engineered to contain a tandem N-terminal HA/His_6 tag in a pET-11d vector. Protein samples were designated monomer or dimer on the basis of their gel-filtration profiles.

Crystallization

Monomer crystals were obtained from 1.2 M NaH_2PO_4/K_2HPO_4, pH 5.5. Se-Met protein crystals were grown from similar conditions with 10 mM β-mercaptoethanol. Dimer

crystals were obtained from 10% (v/v) methyl-2,4-pentanediol (MPD), 18% polyethylene glycol (PEG) 4000 and 0.1 M Tris–HCl, pH 8.4. The native monomer data set was collected at SSRL 9-2 to 2.0 Å resolution, and a three-wavelength MAD data set with Se-Met derivative was collected at ALS 8.2.1 to 2.7 Å. The dimer data set was collected at ALS 5.0.2 to 2.18 Å. All data sets were processed with the program HKL2000.[102] Phases to 2.7 Å were obtained from the MAD data set with the program SOLVE, and density modification was performed by RESOLVE.[103] Phases were extended with the native data set (2.0 Å) with the program DM.[104] The automatic model building program ARP/wARP[105] and manual building were used to build both main chain and side chains from the phase-extended map. The resulting model was initially refined with CNS[106] and completed with REFMAC5 using TLS refinement.[107] Manual model fitting was carried out using the programs O[108] and COOT.[109] The dimer phases were solved from native data set with the molecular replacement program Molrep,[104] using the monomer structure as the search model. The stereochemical quality of the models were verified using AutoDepInputTool[110] MolProbity,[111] and WHATIF 5.0.[112] Data collection and refinement statistics are summarized in Table 1. The dimer crystals have one dimer in the asymmetric unit, while the monomer crystals have one monomer in the asymmetric unit. The dimer configuration cannot be constructed from any of the symmetry operators in the monomer crystal unit cell.

Binding of p115 to Rab1

A 25 μg sample of recombinant GST-Rab1 protein was immobilized to 5 μl of GST beads (GE Healthcare, Piscataway, NJ) in reaction buffer (25 mM Hepes–KOH (pH 7.4), 100 mM NaCl, 1 mM $MgCl_2$, 1 mM DTT) followed by nucleotide exchange with GTPγS or GDP.[37] A 50 μg sample of purified full-length p115 was incubated in the reaction buffer plus 1 mM nucleotide at 4 °C overnight followed by washing three times with reaction buffer. Protein bound to the beads was eluted with denaturing buffer (10 mM Tris–HCl (pH 7.0), 1% (w/v) SDS, 1% β-mercaptoethanol) at 37 °C for 10 min, and analyzed by SDS-PAGE with silver staining to determine purity.

Generation of p115 N-terminal domain mutants

Point mutations in the p115 H1 domain (residues 21–54) were engineered using pFastBAC1-hexaHis-p115 wild type as the template and complimentary mutagenic oligomers with the Quikchange Kit (Stratagene, #200518). Following sequence confirmation, mutagenized p115 fragments (residues 1–456) were excised by digestion with NdeI-Bsu36I and ligated back into the similarly digested FastBAC-His_6-p115 template. DH10BAC. *E. coli* was transposed with the pFastBAC1-His_6-mutant p115 plasmids to generate mutant His_6-p115 bacmids using the BAC-to-BAC Baculovirus Expression System (GibcoBRL/Invitrogen Corp.). Sf9 insect cells were transfected with the bacmids to produce recombinant mutant His_6-p115 baculoviruses, which were then used to infect TN5 insect cells for protein expression.

Transport *in vivo*

[^{35}S]Met pulse–chase labeling and vaccinia transient expression and quantification were as described.[113]

Protein Data Bank accession codes

Coordinates and structure factors have been deposited in the PDB with accession codes 3gq2 (dimer) and 3grl (monomer).

Acknowledgements

This work was supported by grants NIH GM42336 and GM33301 (to W.E.B.), and CA58896 (to I.A.W.). We acknowledge the helpful support of staff members at SSRL 9-2, ALS 8.2.1 and ALS 5.0.2. This is TSRI manuscript #67854.

Supplementary Data

Supplementary data associated with this article can be found, in the online version, at doi:10.1016/j.jmb.2009.04.062

References

1. Gurkan, C., Lapp, H., Alory, C., Su, A. I., Hogenesch, J. B. & Balch, W. E. (2005). Large-scale profiling of Rab GTPase trafficking networks: the membrome. *Mol. Biol. Cell*, **16**, 3847–3864.
2. Sztul, E. & Lupashin, V. (2006). Role of tethering factors in secretory membrane traffic. *Am. J. Physiol. Cell Physiol.* **290**, 11–26.
3. Grosshans, B. L., Ortiz, D. & Novick, P. (2006). Rabs and their effectors: achieving specificity in membrane traffic. *Proc. Natl Acad. Sci. USA*, **103**, 11821–11827.
4. Pfeffer, S. R. (2007). Unsolved mysteries in membrane traffic. *Annu. Rev. Biochem.* **76**, 629–645.
5. Drin, G., Morello, V., Casella, J. F., Gounon, P. & Antonny, B. (2008). Asymmetric tethering of flat and curved lipid membranes by a golgin. *Science*, **320**, 670–673.
6. Diao, A., Frost, L., Morohashi, Y. & Lowe, M. (2008). Coordination of golgin tethering and SNARE assembly: GM130 binds syntaxin 5 in a p115-regulated manner. *J. Biol. Chem.* **283**, 6957–6967.
7. Burguete, A. S., Fenn, T. D., Brunger, A. T. & Pfeffer, S. R. (2008). Rab and Arl GTPase family members cooperate in the localization of the golgin GCC185. *Cell*, **132**, 286–298.
8. Rosing, M., Ossendorf, E., Rak, A. & Barnekow, A. (2007). Giantin interacts with both the small GTPase Rab6 and Rab1. *Exp. Cell Res.* **313**, 2318–2325.
9. Lieu, Z. Z., Derby, M. C., Teasdale, R. D., Hart, C., Gunn, P. & Gleeson, P. A. (2007). The golgin GCC88 is required for efficient retrograde transport of cargo from the early endosomes to the trans-Golgi network. *Mol. Biol. Cell*, **18**, 4979–4991.
10. Derby, M. C., Lieu, Z. Z., Brown, D., Stow, J. L., Goud, B. & Gleeson, P. A. (2007). The trans-Golgi network golgin, GCC185, is required for endosome-to-Golgi transport and maintenance of Golgi structure. *Traffic*, **8**, 758–773.
11. Stefano, G., Renna, L., Hanton, S. L., Chatre, L., Haas, T. A. & Brandizzi, F. (2006). ARL1 plays a role in the binding of the GRIP domain of a peripheral matrix

protein to the Golgi apparatus in plant cells. *Plant Mol. Biol.* **61**, 431–449.
12. Short, B., Haas, A. & Barr, F. A. (2005). Golgins and GTPases, giving identity and structure to the Golgi apparatus. *Biochim. Biophys. Acta*, **1744**, 383–395.
13. Lieu, Z. Z., Lock, J. G., Hammond, L. A., La Gruta, N. L., Stow, J. L. & Gleeson, P. A. (2008). A trans-Golgi network golgin is required for the regulated secretion of TNF in activated macrophages in vivo. *Proc. Natl Acad. Sci. USA*, **105**, 3351–3356.
14. Luke, M. R., Houghton, F., Perugini, M. A. & Gleeson, P. A. (2005). The trans-Golgi network GRIP-domain proteins form α-helical homodimers. *Biochem. J.* **388**, 835–841.
15. Sacher, M., Kim, Y. G., Lavie, A., Oh, B. H. & Segev, N. (2008). The TRAPP complex: insights into its architecture and function. *Traffic*, **9**, 2032–2042.
16. Kummel, D. & Heinemann, U. (2008). Diversity in structure and function of tethering complexes: evidence for different mechanisms in vesicular transport regulation. *Curr. Protein Pept. Sci.* **9**, 197–209.
17. Cai, Y., Chin, H. F., Lazarova, D., Menon, S., Fu, C., Cai, H. *et al.* (2008). The structural basis for activation of the Rab Ypt1p by the TRAPP membrane-tethering complexes. *Cell*, **133**, 1202–1213.
18. Kummel, D., Muller, J. J., Roske, Y., Henke, N. & Heinemann, U. (2006). Structure of the Bet3-Tpc6B core of TRAPP: two Tpc6 paralogs form trimeric complexes with Bet3 and Mum2. *J. Mol. Biol.* **361**, 22–32.
19. Kim, Y. G., Raunser, S., Munger, C., Wagner, J., Song, Y. L., Cygler, M. *et al.* (2006). The architecture of the multisubunit TRAPP I complex suggests a model for vesicle tethering. *Cell*, **127**, 817–830.
20. Kummel, D., Muller, J. J., Roske, Y., Misselwitz, R., Bussow, K. & Heinemann, U. (2005). The structure of the TRAPP subunit TPC6 suggests a model for a TRAPP subcomplex. *EMBO Rep.* **6**, 787–793.
21. Zeevaert, R., Foulquier, F., Jaeken, J. & Matthijs, G. (2008). Deficiencies in subunits of the conserved oligomeric Golgi (COG) complex define a novel group of congenital disorders of glycosylation. *Mol. Genet. Metab.* **93**, 15–21.
22. Chavas, L. M., Ihara, K., Kawasaki, M., Torii, S., Uejima, T., Kato, R. *et al.* (2008). Elucidation of Rab27 recruitment by its effectors: structure of Rab27a bound to Exophilin4/Slp2-a. *Structure*, **16**, 1468–1477.
23. Sohda, M., Misumi, Y., Yoshimura, S., Nakamura, N., Fusano, T., Ogata, S. *et al.* (2007). The interaction of two tethering factors, p115 and COG complex, is required for Golgi integrity. *Traffic*, **8**, 270–284.
24. Cavanaugh, L. F., Chen, X., Richardson, B. C., Ungar, D., Pelczer, I., Rizo, J. & Hughson, F. M. (2007). Structural analysis of conserved oligomeric Golgi complex subunit 2. *J. Biol. Chem.* **282**, 23418–23426.
25. Ungar, D., Oka, T., Krieger, M. & Hughson, F. M. (2006). Retrograde transport on the COG railway. *Trends Cell Biol.* **16**, 113–120.
26. Ungar, D., Oka, T., Vasile, E., Krieger, M. & Hughson, F. M. (2005). Subunit architecture of the conserved oligomeric Golgi complex. *J. Biol. Chem.* **280**, 32729–32735.
27. Lupashin, V. & Sztul, E. (2005). Golgi tethering factors. *Biochim. Biophys. Acta*, **1744**, 325–339.
28. Kawasaki, M., Nakayama, K. & Wakatsuki, S. (2005). Membrane recruitment of effector proteins by Arf and Rab GTPases. *Curr. Opin. Struct. Biol.* **15**, 681–689.
29. Jahn, R. & Scheller, R. H. (2006). SNAREs–engines for membrane fusion. *Nature Rev. Mol. Cell Biol.* **7**, 631–643.
30. Wickner, W. & Schekman, R. (2008). Membrane fusion. *Nature Struct. Mol. Biol*, **15**, 658–664.
31. Dong, G., Medkova, M., Novick, P. & Reinisch, K. M. (2007). A catalytic coiled coil: structural insights into the activation of the Rab GTPase Sec4p by Sec2p. *Mol. Cell*, **25**, 455–462.
32. Shiba, T., Koga, H., Shin, H. W., Kawasaki, M., Kato, R., Nakayama, K. & Wakatsuki, S. (2006). Structural basis for Rab11-dependent membrane recruitment of a family of Rab11-interacting protein 3 (FIP3)/Arfophilin-1. *Proc. Natl Acad. Sci. USA*, **103**, 15416–15421.
33. Waters, M. G., Clary, D. O. & Rothman, J. E. (1992). A novel 115-kD peripheral membrane protein is required for intercisternal transport in the Golgi stack. *J. Cell Biol.* **118**, 1015–1026.
34. Sapperstein, S. K., Walter, D. M., Grosvenor, A. R., Heuser, J. E. & Waters, M. G. (1995). p115 is a general vesicular transport factor related to the yeast endoplasmic reticulum to Golgi transport factor Uso1p. *Proc. Natl Acad. Sci. USA*, **92**, 522–526.
35. Shorter, J., Beard, M. B., Seemann, J., Dirac-Svejstrup, A. B. & Warren, G. (2002). Sequential tethering of Golgins and catalysis of SNAREpin assembly by the vesicle-tethering protein p115. *J. Cell Biol.* **157**, 45–62.
36. Beard, M., Satoh, A., Shorter, J. & Warren, G. (2005). A cryptic Rab1-binding site in the p115 tethering protein. *J. Biol. Chem.* **280**, 25840–25848.
37. Allan, B. B., Moyer, B. D. & Balch, W. E. (2000). Rab1 recruitment of p115 into a cis-SNARE complex: programming budding COPII vesicles for fusion. *Science*, **289**, 444–448.
38. Alvarez, C., Fujita, H., Hubbard, A. & Sztul, E. (1999). ER to Golgi transport: Requirement for p115 at a pre-Golgi VTC stage. *J. Cell Biol.* **147**, 1205–1222.
39. Moyer, B. D., Allan, B. B. & Balch, W. E. (2001). Rab1 interaction with a GM130 effector complex regulates COPII vesicle cis–Golgi tethering. *Traffic*, **2**, 268–276.
40. Nelson, D. S., Alvarez, C., Gao, Y. S., Garcia-Mata, R., Fialkowski, E. & Sztul, E. (1998). The membrane transport factor TAP/p115 cycles between the Golgi and earlier secretory compartments and contains distinct domains required for its localization and function. *J. Cell Biol.* **143**, 319–331.
41. Cao, X., Ballew, N. & Barlowe, C. (1998). Initial docking of ER-derived vesicles requires Uso1p and Ypt1p but is independent of SNARE proteins. *EMBO J.* **17**, 2156–2165.
42. Puthenveedu, M. A. & Linstedt, A. D. (2001). Evidence that Golgi structure depends on a p115 activity that is independent of the vesicle tether components giantin and GM130. *J. Cell Biol.* **155**, 227–238.
43. Sapperstein, S. K., Lupashin, V. V., Schmitt, H. D. & Waters, M. G. (1996). Assembly of the ER to Golgi SNARE complex requires Uso1p. *J. Cell Biol.* **132**, 755–767.
44. Barroso, M., Nelson, D. S. & Sztul, E. (1995). Transcytosis-associated protein (TAP)/p115 is a general fusion factor required for binding of vesicles to acceptor membranes. *Proc. Natl Acad. Sci. USA*, **92**, 527–531.
45. Morsomme, P. & Riezman, H. (2002). The Rab GTPase Ypt1p and tethering factors couple protein

sorting at the ER to vesicle targeting to the Golgi apparatus. *Dev. Cell*, **2**, 307–317.
46. Sohda, M., Misumi, Y., Yoshimura, S., Nakamura, N., Fusano, T., Sakisaka, S. *et al.* (2005). Depletion of vesicle-tethering factor p115 causes mini-stacked Golgi fragments with delayed protein transport. *Biochem. Biophys. Res. Commun.* **338**, 1268–1274.
47. Bentley, M., Liang, Y., Mullen, K., Xu, D., Sztul, E. & Hay, J. C. (2006). SNARE status regulates tether recruitment and function in homotypic COPII vesicle fusion. *J. Biol. Chem.* **281**, 38825–38833.
48. Shorter, J. & Warren, G. (1999). A role for the vesicle tethering protein, p115, in the post-mitotic stacking of reassembling Golgi cisternae in a cell-free system. *J. Cell Biol.* **146**, 57–70.
49. Levine, T. P., Rabouille, C., Kieckbusch, R. H. & Warren, G. (1996). Binding of the vesicle docking protein p115 to Golgi membranes is inhibited under mitotic conditions. *J. Biol. Chem.* **271**, 17304–17311.
50. Nakamura, N., Lowe, M., Levine, T. P., Rabouille, C. & Warren, G. (1997). The vesicle docking protein p115 binds GM130, a cis-Golgi matrix protein, in a mitotically regulated manner. *Cell*, **89**, 445–455.
51. Lesa, G. M., Seemann, J., Shorter, J., Vandekerckhove, J. & Warren, G. (2000). The amino-terminal domain of the golgi protein giantin interacts directly with the vesicle-tethering protein p115. *J. Biol. Chem.* **275**, 2831–2836.
52. Seemann, J., Jokitalo, E. J. & Warren, G. (2000). The role of the tethering proteins p115 and GM130 in transport through the Golgi apparatus in vivo. *Mol. Biol. Cell*, **11**, 635–645.
53. Malsam, J., Satoh, A., Pelletier, L. & Warren, G. (2005). Golgin tethers define subpopulations of COPI vesicles. *Science*, **307**, 1095–1098.
54. Chiu, R., Novikov, L., Mukherjee, S. & Shields, D. (2002). A caspase cleavage fragment of p115 induces fragmentation of the Golgi apparatus and apoptosis. *J. Cell Biol.* **159**, 637–648.
55. Mukherjee, S., Chiu, R., Leung, S. M. & Shields, D. (2007). Fragmentation of the Golgi apparatus: an early apoptotic event independent of the cytoskeleton. *Traffic*, **8**, 369–378.
56. Puthenveedu, M. A. & Linstedt, A. D. (2004). Gene replacement reveals that p115/SNARE interactions are essential for Golgi biogenesis. *Proc. Natl Acad. Sci. USA*, **101**, 1253–1256.
57. Gmachl, M. J. & Wimmer, C. (2001). Sequential involvement of p115, SNAREs, and Rab proteins in intra-Golgi protein transport. *J. Biol. Chem.* **276**, 18178–18184.
58. Kobe, B. & Kajava, A. V. (2000). When protein folding is simplified to protein coiling: the continuum of solenoid protein structures. *Trends Biochem. Sci.* **25**, 509–515.
59. Connolly, M. L. (1993). The molecular surface package. *J. Mol. Graph.* **11**, 139–141.
60. Gelin, B. R. & Karplus, M. (1979). Side-chain torsional potentials: effect of dipeptide, protein, and solvent environment. *Biochemistry (Mosc.)*, **18**, 1256–1268.
61. McDonald, I. K. & Thornton, J. M. (1994). Satisfying hydrogen bonding potential in proteins. *J. Mol. Biol.* **238**, 777–793.
62. Sheriff, S., Hendrickson, W. A. & Smith, J. L. (1987). Structure of myohemerythrin in the azidomet state at 1.7/1.3 Å resolution. *J. Mol. Biol.* **197**, 273–296.
63. Sheriff, S., Silverton, E. W., Padlan, E. A., Cohen, G. H., Smith-Gill, S. J., Finzel, B. C. & Davies, D. R. (1987). Three-dimensional structure of an antibody-antigen complex. *Proc. Natl Acad. Sci. USA*, **84**, 8075–8079.
64. Nicholls, A., Sharp, K. A. & Honig, B. (1991). Protein folding and association: insights from the interfacial and thermodynamic properties of hydrocarbons. *Proteins: Struct. Funct. Genet.* **11**, 281–296.
65. Holm, L. & Sander, C. (1993). Protein structure comparison by alignment of distance matrices. *J. Mol. Biol.* **233**, 123–138.
66. Conti, E. (2002). Structures of importins. *Results Probl. Cell Differ.* **35**, 93–113.
67. Conti, E. & Kuriyan, J. (2000). Crystallographic analysis of the specific yet versatile recognition of distinct nuclear localization signals by karyopherin α. *Structure*, **8**, 329–338.
68. Conti, E., Uy, M., Leighton, L., Blobel, G. & Kuriyan, J. (1998). Crystallographic analysis of the recognition of a nuclear localization signal by the nuclear import factor karyopherin α. *Cell*, **94**, 193–204.
69. Huber, A. H., Nelson, W. J. & Weis, W. I. (1997). Three-dimensional structure of the armadillo repeat region of β-catenin. *Cell*, **90**, 871–882.
70. Shomura, Y., Dragovic, Z., Chang, H. C., Tzvetkov, N., Young, J. C., Brodsky, J. L. *et al.* (2005). Regulation of Hsp70 function by HspBP1: structural analysis reveals an alternate mechanism for Hsp70 nucleotide exchange. *Mol. Cell*, **17**, 367–379.
71. Chook, Y. M. & Blobel, G. (1999). Structure of the nuclear transport complex karyopherin-β2-Ran x GppNHp. *Nature*, **399**, 230–237.
72. Chook, Y. M. & Blobel, G. (2001). Karyopherins and nuclear import. *Curr. Opin. Struct. Biol.* **11**, 703–715.
73. Cingolani, G., Petosa, C., Weis, K. & Muller, C. W. (1999). Structure of importin-β bound to the IBB domain of importin-α. *Nature*, **399**, 221–229.
74. Gruber, M., Soding, J. & Lupas, A. N. (2006). Comparative analysis of coiled-coil prediction methods. *J. Struct. Biol.* **155**, 140–145.
75. McDonnell, A. V., Jiang, T., Keating, A. E. & Berger, B. (2006). Paircoil2: improved prediction of coiled coils from sequence. *Bioinformatics*, **22**, 356–358.
76. Guo, Y., Punj, V., Sengupta, D. & Linstedt, A. D. (2008). Coat-tether interaction in Golgi organization. *Mol. Biol. Cell*, **19**, 2830–2843.
77. Satoh, A. & Warren, G. (2008). In situ cleavage of the acidic domain from the p115 tether inhibits exocytic transport. *Traffic*, **9**, 1522–1529.
78. Aridor, M., Fish, K. N., Bannykh, S., Weissman, J., Roberts, T. H., Lippincott-Schwartz, J. & Balch, W. E. (2001). The Sar1 GTPase coordinates biosynthetic cargo selection with endoplasmic reticulum export site assembly. *J. Cell Biol.* **152**, 213–229.
79. Rowe, T., Aridor, M., McCaffery, J. M., Plutner, H., Nuoffer, C. & Balch, W. E. (1996). COPII vesicles derived from mammalian endoplasmic reticulum microsomes recruit COPI. *J. Cell Biol.* **135**, 895–911.
80. Brown, W. J., Plutner, H., Drecktrah, D., Judson, B. L. & Balch, W. E. (2008). The lysophospholipid acyltransferase antagonist CI-976 inhibits a late step in COPII vesicle budding. *Traffic*, **9**, 786–797.
81. Bannykh, S. I., Plutner, H., Matteson, J. & Balch, W. E. (2005). The role of ARF1 and Rab GTPases in polarization of the Golgi stack. *Traffic*, **6**, 803–819.
82. Aridor, M., Bannykh, S. I., Rowe, T. & Balch, W. E. (1999). Cargo can modulate COPII vesicle formation from the endoplasmic reticulum. *J. Biol. Chem.* **274**, 4389–4399.
83. Huber, A. H. & Weis, W. I. (2001). The structure of the β-catenin/E-cadherin complex and the molecular

basis of diverse ligand recognition by β-catenin. *Cell*, **105**, 391–402.
84. Stewart, M. (2007). Molecular mechanism of the nuclear protein import cycle. *Nature Rev. Mol. Cell Biol.* **8**, 195–208.
85. Goldfarb, D. S., Corbett, A. H., Mason, D. A., Harreman, M. T. & Adam, S. A. (2004). Importin α: a multipurpose nuclear-transport receptor. *Trends Cell Biol.* **14**, 505–514.
86. Harel, A. & Forbes, D. J. (2004). Importin β: conducting a much larger cellular symphony. *Mol. Cell*, **16**, 319–330.
87. Choi, H. J., Huber, A. H. & Weis, W. I. (2006). Thermodynamics of β-catenin-ligand interactions: the roles of the N- and C-terminal tails in modulating binding affinity. *J. Biol. Chem.* **281**, 1027–1038.
88. Sato, Y., Fukai, S., Ishitani, R. & Nureki, O. (2007). Crystal structure of the Sec4p.Sec2p complex in the nucleotide exchanging intermediate state. *Proc. Natl Acad. Sci. USA*, **104**, 8305–8310.
89. Sato, Y., Shirakawa, R., Horiuchi, H., Dohmae, N., Fukai, S. & Nureki, O. (2007). Asymmetric coiled-coil structure with guanine nucleotide exchange activity. *Structure*, **15**, 245–252.
90. Wang, Y., Satoh, A. & Warren, G. (2005). Mapping the functional domains of the Golgi stacking factor GRASP65. *J. Biol. Chem.* **280**, 4921–4928.
91. Satoh, A., Malsam, J. & Warren, G. (2005). Tethering assays for COPI vesicles mediated by golgins. *Methods Enzymol.* **404**, 125–134.
92. Hayes, G. L., Brown, F. C., Haas, A. K., Nottingham, R. M., Barr, F. A. & Pfeffer, S. R. (2009). Multiple Rab GTPase binding sites in GCC185 suggest a model for vesicle tethering at the trans-Golgi. *Mol. Biol. Cell*, **20**, 209–217.
93. Wu, M., Lu, L., Hong, W. & Song, H. (2004). Structural basis for recruitment of GRIP domain golgin-245 by small GTPase Arl1. *Nature Struct. Mol. Biol.* **11**, 86–94.
94. Panic, B., Perisic, O., Veprintsev, D. B., Williams, R. L. & Munro, S. (2003). Structural basis for Arl1-dependent targeting of homodimeric GRIP domains to the Golgi apparatus. *Mol. Cell*, **12**, 863–874.
95. Wennerberg, K., Rossman, K. L. & Der, C. J. (2005). The Ras superfamily at a glance. *J. Cell Sci.* **118**, 843–846.
96. Colicelli, J. (2004). Human RAS superfamily proteins and related GTPases.*Sci. STKE*, **2004**; RE13.
97. Pfeffer, S. R. (2005). Structural clues to Rab GTPase functional diversity. *J. Biol. Chem.* **280**, 15485–15488.
98. Goody, R. S., Rak, A. & Alexandrov, K. (2005). The structural and mechanistic basis for recycling of Rab proteins between membrane compartments. *Cell Mol. Life Sci.* **62**, 1657–1670.
99. Linstedt, A. D., Jesch, S. A., Mehta, A., Lee, T. H., Garcia-Mata, R., Nelson, D. S. & Sztul, E. (2000). Binding relationships of membrane tethering components. The giantin N terminus and the GM130 N terminus compete for binding to the p115 C terminus. *J. Biol. Chem.* **275**, 10196–10201.
100. Sonnichsen, B., Lowe, M., Levine, T., Jamsa, E., Dirac-Svejstrup, B. & Warren, G. (1998). A role for giantin in docking COPI vesicles to Golgi membranes. *J. Cell Biol.* **140**, 1013–1021.
101. Orci, L., Perrelet, A. & Rothman, J. E. (1998). Vesicles on strings: morphological evidence for processive transport within the Golgi stack. *Proc. Natl Acad. Sci. USA*, **95**, 2279–2283.
102. Otwinowski, Z. & Minor, W. (1997). Processing of X-ray diffraction data collected in oscillation mode. *Methods Enzymol.* **276**, 307–326.
103. Terwilliger, T. C. (2003). SOLVE and RESOLVE: automated structure solution and density modification. *Methods Enzymol.* **374**, 22–37.
104. Collaborative Computational Project, Number 4. (1994). The CCP4 suite: programs for protein crystallography. *Acta Crystallogr. D*, **50**, 760–763.
105. Perrakis, A., Morris, R. & Lamzin, V. S. (1999). Automated protein model building combined with iterative structure refinement. *Nature Struct. Biol.* **6**, 458–463.
106. Brunger, A. T., Adams, P. D., Clore, G. M., DeLano, W. L., Gros, P., Grosse-Kunstleve, R. W. *et al.* (1998). Crystallography & NMR system: a new software suite for macromolecular structure determination. *Acta Crystallogr. D*, **54**, 905–921.
107. Winn, M. D., Murshudov, G. N. & Papiz, M. Z. (2003). Macromolecular TLS refinement in REFMAC at moderate resolutions. *Methods Enzymol.* **374**, 300–321.
108. Jones, T. A., Zou, J. Y., Cowan, S. W. & Kjeldgaard (1991). Improved methods for building protein models in electron density maps and the location of errors in these models. *Acta Crystallogr. A*, **47**, 110–119.
109. Emsley, P. & Cowtan, K. (2004). Coot: model-building tools for molecular graphics. *Acta Crystallogr. D*, **60**, 2126–2132.
110. Yang, H., Guranovic, V., Dutta, S., Feng, Z., Berman, H. M. & Westbrook, J. D. (2004). Automated and accurate deposition of structures solved by X-ray diffraction to the Protein Data Bank. *Acta Crystallogr. D*, **60**, 1833–1839.
111. Davis, I. W., Murray, L. W., Richardson, J. S. & Richardson, D. C. (2004). MOLPROBITY: structure validation and all-atom contact analysis for nucleic acids and their complexes. *Nucleic Acids Res*, **32**, W615–W619.
112. Vriend, G. (1990). WHAT IF: a molecular modeling and drug design program. *J. Mol. Graph.* **8**, 52–56.
113. Yoo, J. S., Moyer, B. D., Bannykh, S., Yoo, H. M., Riordan, J. R. & Balch, W. E. (2002). Non-conventional trafficking of the cystic fibrosis transmembrane conductance regulator through the early secretory pathway. *J. Biol. Chem.* **277**, 11401–11409.
114. Kraulis, P. J. (1991). MOLSCRIPT: A program to produce both detailed and schematic plots of protein structures. *J. Appl. Crystallogr.* **24**, 946–950.
115. Merritt, E. A. & Bacon, D. J. (1997). Raster3D: photorealistic molecular graphics. *Methods Enzymol.* **277**, 505–524.
116. Alvarez, C., Garcia-Mata, R., Hauri, H. P. & Sztul, E. (2001). The p115-interactive proteins GM130 and giantin participate in endoplasmic reticulum-Golgi traffic. *J. Biol. Chem.* **276**, 2693–2700.

Note added in proof. A crystal structure of the p115 globular head was reported by Striegl, H., Roske, Y., Kümmel, D., Heinemann, U. (2009). *PLoS ONE*, **4**, e4656. The features in that structure are very similar to those reported here.